MATCH
Communications in Mathematical and in Computer Chemistry

MATCH Commun. Math. Comput. Chem. **91** (2024) 415–452
ISSN: 0340–6253
doi: 10.46793/match.91-2.415K

Codimension-One and Codimension-Two Bifurcations of a Fractional-Order Cubic Autocatalator Chemical Reaction System

Muhammad Asif Khan[a,*], **Qamar Din**[b]

[a] *Department of Mathematics, Kahuta-Haveli Campus, University of Poonch Rawalakot, Azad Kashmir, Pakistan*

[b] *Department of Mathematics, University of Poonch Rawalakot, Azad Kashmir, Pakistan*

asif31182@gmail.com, qamar.sms@gmail.com

(Received July 14, 2023)

Abstract

This article delves into an investigation of the dynamic behavior exhibited by a fractional order cubic autocatalator chemical reaction model. Specifically, our focus lies on exploring codimension-one bifurcations associated with period-doubling bifurcation and Neimark-Sacker bifurcation. Additionally, we undertake an analysis of codimension-two bifurcations linked to resonances of the types 1:2, 1:3, and 1:4. To achieve these outcomes, we employ the normal form method and bifurcation theory. The results are presented through comprehensive numerical simulations, encompassing visual representations such as phase portraits, two-parameter bifurcation diagrams, and maximum Lyapunov exponents diagrams. These simulations aptly examine the behavior of a system governed by two distinct parameters that vary within a three-dimensional space. Furthermore, the simulations effectively illustrate the theoretical findings while providing valuable insights into the underlying dynamics.

*Corresponding author.

1 Introduction

Chemical processes involving chemical reactions, mass transfer, heat, fluid flow, and separations exhibit significant nonlinearity, leading to complexity. To maintain stability and control over the process conditions, process engineers prescribe homogeneous properties for the product obtained. The inherent nonlinearity of the chemical reaction results in sudden complexity during the industrial process, even in the absence of external disturbances. Over the past decade, there has been a notable increase in the publication of articles pertaining to processes that exhibit oscillatory behavior, multiple fixed points, and chaos [2, 18, 25].

For more than a century, the study of oscillatory behavior in chemical reactions has been of great interest to both experimentalists and theoreticians. Notable examples of oscillatory systems in chemical engineering and thermodynamics include the Belousov-Zhabotinsky, Bray-Liebhafsky, and Briggs-Rausher reactions. These reactions exhibit oscillatory behavior in concentration, which is observable through changes in color [15]. The continuous flow well-stirred tank reactor (CSTR), also referred to as a backmix reactor or vat, is a commonly used reactor for studying chemical dynamics, as reported in the literature [22]. During experiments, the system of ordinary differential equations governing the CSTR can be managed using standard techniques.

Furthermore, numerous studies have demonstrated that CSTRs can exhibit a rich variety of dynamic phenomena, with fluctuations being a feature of particular interest to both chemical engineers and mathematicians [3]. Investigations into self-oscillatory CSTRs have led to two distinct directions: one involves eliminating oscillations, while the other takes advantage of process dynamics for unsteady-state operation [2, 18, 25]. An optimal model would go beyond conventional fixed-point optimization by incorporating time-evolution, which offers opportunities for enhancing process efficiency through cyclic processes.

The combination of two oscillatory CSTRs has been shown to generate chaos [7, 8, 41]. Bifurcation analysis of steady-state is used to explore the complex dynamical behavior of CSTRs. This analysis not only examines the unforced system but also assesses the dynamic complexities that arise when periodic forcing is introduced. Classic methodical tools, such as codimension-1 bifurcations of limit cycles and stroboscopic Poincare maps [24], are employed to study chaos that frequently occurs in CSTRs during period-doubling and Neimark-Sacker bifurcations.

The Bclousov-Zhabotinskil (BZ) reaction, one of the most well-known chemical reactions, was first mathematically modeled by Field and Noyes [38] under isothermal conditions. Leach et al. [19] demonstrated the existence of Hopf bifurcation in a two-cell coupled cubic autocatalator chemical reaction model. In [21], the author explored the presence of limit cycles in a cubic chemical autocatalator model and found that they exist within a restricted parameter space. In [14], the author studied a cubic autocatalator chemical reaction model and determined that traveling waves do not occur unless the initial concentration of reactant is periodic. In [30] author investigated a reaction of a homogeneous-heterogeneous nano-fluid and found evidence of hysteresis bifurcations and multiple solutions. Alderremy et al. [1] proposed a new fractional blood ethanol model and briefly compared it with the fractional-cubic autocatalator reaction model. Kay and Scott [26], as well as [5, 39], demonstrated that these reactions exhibit oscillatory behavior in exothermic conditions. Gray and Scott [27] introduced a cubic autocatalator chemical reaction model that displays oscillatory behavior, which is governed by the following reaction steps:

$$P \xrightarrow{c_0} L,\ 2M \xrightarrow{c_1} 3M,\ M \xrightarrow{c_2} N, L \xrightarrow{c_3} M, \tag{1}$$

where $c_0, \cdots, c_3$ are constants, $p,\ l,\ m, n$ are the molar concentrations of chemical species $P, L,\ M$ and N, respectively. Based on the assumption of isothermal reaction, we have the following 2-dimensional system:

$$\begin{aligned} \frac{dl}{dt} &= c_0 p - c_1 l m^2 - c_3 l, \\ \frac{dm}{dt} &= c_1 l m^2 - c_2 l + c_3 l. \end{aligned} \tag{2}$$

On the other hand, the dimensionless version of (2) is given by [20, 31]:

$$\begin{aligned} \frac{dx}{dt} &= \mu - x y^2 - r x, \\ \frac{dy}{dt} &= x y^2 - y + r x, \end{aligned} \tag{3}$$

where $\mu,\ r > 0$. Merkin et al. [16] performed a comprehensive analysis of system (3). In [17], the authors focused on the specific case of model (3), where $r = 0$ and demonstrated the presence of periodic behavior for the parameter μ. Gray and Thuraisingham [6] introduced additional parameters to system (3) and examined its bifurcation analysis. In addition, Forbes and Holmes [20] investigated the limit cycle behavior of system (3). Notice that, unlike traditional integer order models, fractional order models incorporate fractional derivatives in their formulation, which can provide a more accurate description of the reaction kinetics. These models are used to better understand the underlying mechanisms of chemical reactions, optimize chemical processes, and develop new materials and technologies. They are also being used in medical applications to model drug delivery systems and study physiological processes. Overall, fractional order chemical reaction models are a powerful tool in the field of chemistry and related disciplines [23]. For further reading on mathematical models concerning chemical reactions in both continuous and discrete frameworks, the reader is encouraged to consult references [32–37].

Taking into account the facts that fractional calculus allows more accurate modeling of complex systems which cannot be described by integer-order differential systems, and the fractional system can be adapted to fit a variety of data sets, it is more appropriate to consider the fractional-order counterpart of the system (3).

Prior to transforming system (3) into its fractional-order counterpart, we review some necessary concepts from fractional calculus as follows [4]:

The Caputo fractional-order derivative is a generalization of the classical derivative to non-integer orders. It is defined as follows:

Let $\alpha > 0$ be a real number and $m-1 < \alpha < m \in \mathbb{Z}^+$. Let $f : [0, \infty) \to \mathbb{R}$ be a continuous function that is m times differentiable on $(0, \infty)$. Then, the Caputo fractional-order derivative of order α of f at $t > 0$ is given by:

$$D^\alpha f(t) = \frac{1}{\Gamma(m-\alpha)} \int_0^t \frac{f^{(m)}(\tau)}{(t-\tau)^{\alpha-m+1}} d\tau, \tag{4}$$

where $f^{(m)}$ is the m-th classical derivative of f, and $\Gamma(\cdot)$ denotes the Euler's

Gamma function defined as:

$$\Gamma(z) := \int_0^\infty e^{-t} t^{z-1} dt, \ z \in \mathbb{C}, \ Re(z) > 0.$$

Moreover, the Riemann-Liouville integral operator I^ϑ of order ϑ is defined as follows:

$$I^\vartheta g(t) = \frac{1}{\Gamma(\vartheta)} \int_0^t (t-s)^{\vartheta-1} g(s) ds, \ \vartheta > 0. \tag{5}$$

Here, we use the Caputo fractional-order derivative because it has some advantages over other definitions, such as:

- It preserves the initial conditions of the system, meaning that the values of the state variables and their integer-order derivatives at $t = 0$ are well-defined and consistent with the classical case.
- It allows for a smooth transition from the fractional-order system to the integer-order system when fractional-order approaches an integer value.
- It is more suitable for modeling physical phenomena that involve memory and nonlocal effects.

Next, the fractional-order counterpart of the system (3) is given by:

$$\begin{aligned} D^\alpha x(t) &= \mu - x(t)y^2(t) - rx(t), \\ D^\alpha y(t) &= x(t)y^2(t) - y(t) + rx(t), \end{aligned} \tag{6}$$

where $t > 0$, and α is the fractional order which satisfy $0 < \alpha \leq 1$. There are several ways to discretize this type of system using different techniques. An instance of such methods is the piecewise constant approximation, which involves discretizing the model through the following process. Take into account the initial conditions of the system (6) are $x(0) = x_0$, $y(0) = y_0$. Then system (6) can be discretized as follow:

$$\begin{aligned} D^\alpha x(t) &= \mu - x\left([\tfrac{t}{\rho}]\rho\right) y^2\left([\tfrac{t}{\rho}]\rho\right) - rx\left([\tfrac{t}{\rho}]\rho\right), \\ D^\alpha y(t) &= x\left([\tfrac{t}{\rho}]\rho\right) y^2\left([\tfrac{t}{\rho}]\rho\right) - y\left([\tfrac{t}{\rho}]\rho\right) + rx(\left([\tfrac{t}{\rho}]\rho\right). \end{aligned} \tag{7}$$

Consider $t \in [0, \rho)$, thus $\frac{t}{\rho} \in [0, 1)$. Therefore, we obtain that:

$$\begin{aligned} D^{\alpha}x_1(t) &= \mu - x_0y_0^2 - rx_0, \\ D^{\alpha}y_1(t) &= x_0y_0^2 - y_0 + rx_0. \end{aligned} \tag{8}$$

The solution to equation (8) is given by:

$$\begin{aligned} x_1(t) &= x_0 + I^{\alpha}\left(\mu - x_0y_0^2 - rx_0\right), \\ y_1(t) &= y_0 + I^{\alpha}\left(x_0y_0^2 - y_0 + rx_0\right). \end{aligned} \tag{9}$$

Then, it follows that:

$$\begin{aligned} x_1(t) &= x_0 + \frac{t^{\alpha}}{\Gamma(\alpha+1)}\left(\mu - x_0y_0^2 - rx_0\right), \\ y_1(t) &= y_0 + \frac{t^{\alpha}}{\Gamma(\alpha+1)}\left(x_0y_0^2 - y_0 + rx_0\right). \end{aligned} \tag{10}$$

Next, for $t \in [\rho, 2\rho)$, and taking $\frac{t}{\rho} \in [1, 2)$. Then, one has

$$\begin{aligned} D^{\alpha}x_2(t) &= \mu - x_1y_1^2 - rx_1, \\ D^{\alpha}y_2(t) &= x_1y_1^2 - y_1 + rx_1. \end{aligned} \tag{11}$$

On simplification, one has

$$\begin{aligned} x_2(t) &= x_1(\rho) + \frac{(t-\rho)^{\alpha}}{\Gamma(\alpha+1)}\left(\mu - x_1y_1^2 - rx_1\right), \\ y_2(t) &= y_1(\rho) + \frac{(t-\rho)^{\alpha}}{\Gamma(\alpha+1)}\left(x_1y_1^2 - y_1 + rx_1\right). \end{aligned} \tag{12}$$

Upon iterating the discretization process n-times, we obtain

$$\begin{aligned} x_{n+1}(t) &= x_n(n\rho) + \frac{(t-n\rho)^{\alpha}}{\Gamma(\alpha+1)}\left(\mu - x_n(n\rho)y_n^2(n\rho) - rx_n(n\rho)\right), \\ y_{n+1}(t) &= y_n(n\rho) + \frac{(t-n\rho)^{\alpha}}{\Gamma(\alpha+1)}\left(x_n(n\rho)y_n^2(n\rho) - y_n(n\rho) + rx_n(n\rho)\right), \end{aligned} \tag{13}$$

where $t \in [n\rho, (n+1)\rho)$. For $t \to (n+1)\rho$, we have the following form of system (13):

$$\begin{aligned} x_{n+1} &= x_n + \frac{\rho^{\alpha}}{\Gamma(\alpha+1)}\left[\mu - rx_n - x_ny_n^2\right], \\ y_{n+1} &= y_n + \frac{\rho^{\alpha}}{\Gamma(\alpha+1)}\left[x_ny_n^2 - y_n + rx_n\right], \end{aligned} \tag{14}$$

where $0 < \alpha \leq 1$ is the order of fractional derivative, and $\rho > 0$ is step size for the discretization.

The novel contributions of this paper are outlined as follows:

- The fractional-order nature of the model introduces a new dimension to chemical kinetics. Fractional-order derivatives and integrals provide a more accurate description of reaction rates and system dynamics, enabling a better representation of real-world phenomena.

- The discretization of the fractional-order cubic autocatalator model is crucial for performing numerical simulations and analyses. Discretization methods allow researchers to transform the continuous fractional-order differential equations into discrete equations that can be solved numerically. This facilitates the study of system behavior, stability, bifurcations, and other properties using computational techniques.

- In the fractional-order cubic autocatalator chemical reaction model, codimension-two bifurcations play a significant role in understanding the complex dynamics of the system. Codimension-two bifurcations involve the simultaneous occurrence of two different types of bifurcations, resulting in a higher level of complexity in the system's behavior.

- In the context of the fractional-order cubic autocatalator model, examples of codimension-two bifurcations include 1:2 resonance, 1:3 resonance, and 1:4 resonance. These resonances refer to specific relationships between the frequencies of two or more oscillatory components in the system.

The rest of this paper is structured as follows:

The existence of fixed point and local stability of system (14) is investigated in Section 2. Co-dimension-1 bifurcations (that is, period-doubling bifurcation and Neimark-Sacker bifurcation) are discussed in Section 3. In Section 4, codimension-2 bifurcations are investigated. Finally, in Section 5 numerical simulations are presented.

2 Local stability analysis

It is easy to see that system Eq. 14 has unique positive fixed point $E(x_*, y_*) = (\frac{\mu}{\mu^2+r}, \mu)$.

Subsequently, we examine the local stability analysis of $E(x_*, y_*) = (\frac{\mu}{\mu^2+r}, \mu)$ of system Eq. 14.

To investigate the stability, we compute the Jacobian matrix F_J of system (14) at $E(x_*, y_*)$ as follow:

$$F_J(E) = \begin{pmatrix} 1 - \frac{(\mu^2+r)\rho^\alpha}{\Gamma(\alpha+1)} & -\frac{2\mu^2\rho^\alpha}{(\mu^2+r)\Gamma(\alpha+1)} \\ \frac{(\mu^2+r)\rho^\alpha}{\Gamma(\alpha+1)} & \frac{(\mu^2-r)\rho^\alpha}{(\mu^2+r)\Gamma(\alpha+1)} + 1 \end{pmatrix}$$

The characteristic polynomial of F_J at $E(x_*, y_*)$ is given by:

$$\mathbb{P}(\lambda) = \lambda^2 - A_1(E)\lambda + A_2(E), \tag{15}$$

where

$$A_1(E) = 2 - \frac{\rho^\alpha\left(\mu^4 + \mu^2(2r-1) + r(r+1)\right)}{\Gamma(\alpha+1)\left(\mu^2+r\right)},$$

and

$$A_2(E) = \frac{\rho^\alpha\left(\rho^\alpha\left(\mu^2+r\right)^2 - \Gamma(\alpha+1)\left(\mu^4+\mu^2(2r-1)+r(r+1)\right)\right)}{\Gamma(\alpha+1)^2\left(\mu^2+r\right)} + 1.$$

The following Lemma is used to explore the stability of fixed point.

Lemma 1. *Let $\mathbb{F}(\lambda) = \lambda^2 - A_1(E)\lambda + A_2(E)$, and $\mathbb{P}(1) > 0$. Moreover, λ_1, λ_2 are root of 15, then:*
(i) $|\lambda_1| < 1$ and $|\lambda_2| < 1$ if and only if $\mathbb{P}(-1) > 0$ and $A_2(E) < 1$;
(ii)$|\lambda_1| < 1$ and $|\lambda_2| > 1$ or ($|\lambda_1| > 1$ and $|\lambda_2 < |1$)if and only if $\mathbb{P}(-1) < 0$;
(iii) $|\lambda_1| > 1$ and $|\lambda_2| > 1$ if and only if $\mathbb{P}(-1) > 0$ and $A_2(E) > 1$;
(iv) $\lambda_1 = -1$ and $|\lambda_2| \neq 1$ if and only if $\mathbb{P}(-1) = 0$ and $A_1(E) \neq 0, 2$;
(v) λ_1 and λ_2 are complex and $|\lambda_1| = 1$ and $|\lambda_2| = 1$ if and only if $A_1(E)^2 - 4A_2(E) < 0$ and $A_2(E) = 1$.

As λ_1 and λ_2 are eigenvalue of (15), we have the following Topological *type results. The fixed point $E(x_*, y_*)$ is known as sink if $|\lambda_1| < 1$ and $|\lambda_2| < 1$ thus the sink is locally asymptotic stable. The fixed point$E(x_*, y_*)$ is known as source if $|\lambda_1| > 1$ and $|\lambda_2| > 1$, thus source is always unstable. The fixed point $E(x_*, y_*)$ is known as saddle point if $|\lambda_1| < 1$ and $|\lambda_2| > 1$ or ($|\lambda_1| > 1$ and $|\lambda_2| < 1$) and the fixed point $E(x_*, y_*)$ is known as non-hyperbolic fixed point either $|\lambda_1| = 1$ and $|\lambda_2| = 1$.*

Thus, by applying Lemma 1, we study the local stability of positive equilibrium point of system (14) by stating the following proposition.

Proposition 1. *The positive equilibrium point $E(x_*, y_*)$ of system (14) satisfies the following results.*

(i) The positive fixed point $E(x_*, y_*)$ is sink if and only if:

$$\frac{\rho^\alpha \left(\rho^\alpha \left(\mu^2 + r\right)^2 - 2\Gamma(\alpha+1)\left(\mu^4 + \mu^2(2r-1) + r(r+1)\right)\right)}{\Gamma(\alpha+1)^2 \left(\mu^2 + r\right)} + 4 > 0,$$

and

$$\Gamma(\alpha+1)\left(\mu^4 + \mu^2(2r-1) + r(r+1)\right) > \rho^\alpha \left(\mu^2 + r\right)^2.$$

(ii) The positive fixed point $E(x_*, y_*)$ is saddle point if and only if:

$$\frac{\rho^\alpha \left(\rho^\alpha \left(\mu^2 + r\right)^2 - 2\Gamma(\alpha+1)\left(\mu^4 + \mu^2(2r-1) + r(r+1)\right)\right)}{\Gamma(\alpha+1)^2 \left(\mu^2 + r\right)} + 4 < 0.$$

(iii) The positive fixed point $E(x_*, y_*)$ is source if and only if:

$$\frac{\rho^\alpha \left(\rho^\alpha \left(\mu^2 + r\right)^2 - 2\Gamma(\alpha+1)\left(\mu^4 + \mu^2(2r-1) + r(r+1)\right)\right)}{\Gamma(\alpha+1)^2 \left(\mu^2 + r\right)} + 4 > 0,$$

and

$$\Gamma(\alpha+1)\left(\mu^4 + \mu^2(2r-1) + r(r+1)\right) < \rho^\alpha \left(\mu^2 + r\right)^2.$$

(iv) The positive fixed point $E(x_*, y_*)$ is non-hyperbolic if and only if:

$$\begin{cases} r = \frac{\rho^{-\alpha}\sqrt{\Gamma(\alpha+1)(-(\rho^\alpha-2\Gamma(\alpha+1)))(4\mu^2\rho^{2\alpha}+\rho^\alpha(-\Gamma(\alpha+1))+2\Gamma(\alpha+1)^2)}}{2\Gamma(\alpha+1)} \\ -\frac{\sqrt{\Gamma(\alpha+1)(-(\rho^\alpha-2\Gamma(\alpha+1)))(4\mu^2\rho^{2\alpha}+\rho^\alpha(-\Gamma(\alpha+1))+2\Gamma(\alpha+1)^2)}}{2\Gamma(\alpha+1)(\rho^\alpha-2\Gamma(\alpha+1))} \\ -\rho^{-\alpha}\Gamma(\alpha+1)+\mu^2, \\ and \\ 2-\frac{\rho^\alpha\left(\mu^4+\mu^2(2r-1)+r(r+1)\right)}{\Gamma(\alpha+1)(\mu^2+r)} \neq 0, 2. \end{cases} \tag{16}$$

0r

$$\begin{cases} r = -\frac{2\mu^2\rho^\alpha+\sqrt{\Gamma(\alpha+1)((8\mu^2+1)\Gamma(\alpha+1)-8\mu^2\rho^\alpha)}+\left(-2\mu^2-1\right)\Gamma(\alpha+1)}{2(\rho^\alpha-\Gamma(\alpha+1))}, \\ and \\ 0 < \frac{\rho^\alpha\left(\mu^4+\mu^2(2r-1)+r(r+1)\right)}{\Gamma(\alpha+1)(\mu^2+r)} < 4. \end{cases} \tag{17}$$

Furthermore, for $r \in [0,\ 3]$, $\mu \in [0,\ 3]$ and fixed $(\alpha,\ \rho) = (0.3,\ 0.6)$, the topological classification of system (14) is depicted in Figure 1.

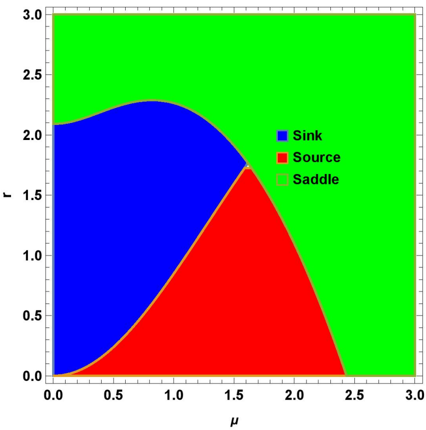

Figure 1. Topological classification for the system (14).

In next section we investigate existence and direction of bifurcation.

3 Codimension-one bifurcations

First, we explore the flip bifurcation of positive fixed point (x_*, y_*) of map (14). In order to study the flip bifurcation assume that

Assume that

$$T_{PB} = \{(\alpha, \rho, \mu, r) \in R_+^4 : (16)\ satisfied\}.$$

The positive fixed point (x_*, y_*) of map (14) undergoes flip bifurcation when parameters vary in a small neighborhood of T_{PB}. Thus map (14) along with parameters $(\alpha, \rho, \mu, r_1) \in T_{PB}$ can be written as follow:

$$\begin{pmatrix} x \\ y \end{pmatrix} \to \begin{pmatrix} x + \frac{\rho^\alpha}{\Gamma(\alpha+1)}\left[\mu - r_1 x - xy^2\right] \\ y + \frac{\rho^\alpha}{\Gamma(\alpha+1)}\left[xy^2 - y + r_1 x\right] \end{pmatrix}. \tag{18}$$

The following perturbation of system (18) can be obtained by taking $\bar{r}$ as bifurcation parameter;

$$\begin{pmatrix} x \\ y \end{pmatrix} \to \begin{pmatrix} x + \frac{\rho^\alpha}{\Gamma(\alpha+1)}\left[\mu - (r_1+\bar{r}) x - xy^2\right] \\ y + \frac{\rho^\alpha}{\Gamma(\alpha+1)}\left[xy^2 - y + (r_1+\bar{r}) x\right] \end{pmatrix}, \tag{19}$$

where $|\bar{r}| << 1$ is a least perturbation parameter. Assuming that $H = x - x_*,\ P = y - y_*$, then system (19) is converted into the following form:

$$\begin{pmatrix} H \\ P \end{pmatrix} \to \begin{pmatrix} a_{11} & a_{12} \\ a_{21} & a_{22} \end{pmatrix}\begin{pmatrix} H \\ P \end{pmatrix} + \begin{pmatrix} f_1(H,P,\bar{r}) \\ f_2(H,P,\bar{r}) \end{pmatrix}, \tag{20}$$

where

$$\begin{aligned} f_1(H,P,\bar{r}) &= a_{13}HP^2 + a_{14}HP + a_{15}P^2 + e_1\bar{r}H \\ &+ e_2\bar{r}P + O\left((|H| + |P| + |\bar{r}|)^4\right), \\ f_2(H,P,\bar{r}) &= b_{13}HP^2 + b_{14}HP + b_{15}P^2 + e_3\bar{r}H \\ &+ O\left((|H| + |P| + |\bar{r}|)^4\right), \end{aligned}$$

where

$$
\begin{aligned}
a_{11} &= 1-\frac{\rho^{\alpha}\left(\mu^{2}+r_{1}\right)}{\Gamma(\alpha+1)},\ a_{12}=-\frac{2\mu^{2}\rho^{\alpha}}{\Gamma(\alpha+1)\left(\mu^{2}+r_{1}\right)},\\
a_{21} &= \frac{\rho^{\alpha}\left(\mu^{2}+r_{1}\right)}{\Gamma(\alpha+1)},\ a_{22}=\frac{\rho^{\alpha}\left(\mu^{2}-r_{1}\right)}{\Gamma(\alpha+1)\left(\mu^{2}+r_{1}\right)}+1,\\
a_{13} &= -\frac{\rho^{\alpha}}{\Gamma(\alpha+1)},\ a_{14}=-\frac{2\mu\rho^{\alpha}}{\Gamma(\alpha+1)},\ b_{13}=\frac{\rho^{\alpha}}{\Gamma(\alpha+1)},\\
e_{1} &= -\frac{\rho^{\alpha}}{\Gamma(\alpha+1)},\ e_{2}=\frac{2\mu^{2}\rho^{\alpha}}{\Gamma(\alpha+1)\left(\mu^{2}+r_{1}\right)^{2}},\\
e_{3} &= \frac{\rho^{\alpha}}{\Gamma(\alpha+1)},\ a_{15}=-\frac{\mu\rho^{\alpha}}{\Gamma(\alpha+1)\left(\mu^{2}+r_{1}\right)},\\
b_{14} &= \frac{2\mu\rho^{\alpha}}{\Gamma(\alpha+1)},\ b_{15}=\frac{\mu\rho^{\alpha}}{\Gamma(\alpha+1)\left(\mu^{2}+r_{1}\right)}.
\end{aligned}
$$

The canonical form of (20) at $r=0$, can be obtained by assuming the following map:

$$
\begin{pmatrix} H \\ P \end{pmatrix}=\begin{pmatrix} a_{12} & a_{12} \\ -1-a_{11} & \lambda_{2}-a_{11} \end{pmatrix}\begin{pmatrix} u \\ v \end{pmatrix}. \tag{21}
$$

The normal form of system (20) under translation (21) can be expressed as:

$$
\begin{pmatrix} u \\ v \end{pmatrix}\rightarrow\begin{pmatrix} -1 & 0 \\ 0 & \lambda_{2} \end{pmatrix}\begin{pmatrix} u \\ v \end{pmatrix}+\begin{pmatrix} \frac{(\lambda_{2}-a_{11})f_{1}}{a_{12}(\lambda_{2}+1)}-\frac{f_{2}}{\lambda_{2}+1} \\ \frac{(1+a_{11})f_{1}}{a_{12}(\lambda_{2}+1)}+\frac{f_{2}}{\lambda_{2}+1} \end{pmatrix}, \tag{22}
$$

where

where, $H=a_{12}\,(u+v)$ and $P=-(1+a_{11})u+(\lambda_{2}-a_{11})\,v$.

Thus approximation of center manifold $W^{c}(0,0,0)$ of (22) in the least neighborhood of $\bar{r}=0$ evaluated at origin can be expressed as:

$$
W^{c}(0,0,0)=\{(u,v,\bar{r}\in R^{3}):v=s_{3}\bar{r}^{2}+s_{2}\bar{r}u+s_{1}u^{2}+(O|u|,|\bar{r}|)^{4}\},
$$

where

$$
\begin{aligned}
s_1 &= \frac{1}{\lambda_2 - 1}\left(\left(\frac{(1+a_{11})\,a_{14}}{a_{12}\,(\lambda_2+1)} + \frac{b_{14}}{\lambda_2+1}\right) a_{12}\,(1+a_{11})\right) \\
&+ \frac{1}{\lambda_2 - 1}\left(\left(\frac{(1+a_{11})\,a_{15}}{a_{12}\,(\lambda_2+1)} + \frac{b_{15}}{\lambda_2+1}\right) (1+a_{11})^2\right), \\
s_2 &= \frac{1}{1-\lambda_2}\left(\left(\frac{(1+a_{11})\,e_1}{a_{12}\,(\lambda_2+1)} + \frac{e_3}{\lambda_2+1}\right) a_{12}\right) \\
&- \frac{1}{1-\lambda_2}\left(\frac{(1+a_{11})\,e_2\,(1+a_{11})}{a_{12}\,(\lambda_2+1)}\right), \ s_3 = 0.
\end{aligned}
$$

Hence, the map restricted to the center manifold $W^c(0,0,0)$ is expressed as:

$$
F : u \to -u + t_1 u^2 + t_2 u\bar{r} + t_3 u^2\bar{r} + k_4 u\bar{r}^2 + k_5 u^3 + (O|u|, |\bar{r}|)^4,
$$

where

$$
\begin{aligned}
t_1 &= \left(\frac{(a_{11}-\lambda_2)\,a_{14}}{a_{12}\,(\lambda_2+1)} - \frac{b_{14}}{\lambda_2+1}\right) a_{12}\,(1+a_{11}) \\
&+ \left(\frac{(\lambda_2-a_{11})\,a_{15}}{a_{12}\,(\lambda_2+1)} - \frac{b_{15}}{\lambda_2+1}\right) (1+a_{11})^2, \\
t_2 &= \left(\frac{(\lambda_2-a_{11})\,e_1}{a_{12}\,(\lambda_2+1)} + \frac{e_3}{\lambda_2+1}\right) a_{12} - \frac{(\lambda_2-a_{11})\,e_2\,(1+a_{11})}{a_{12}\,(\lambda_2+1)}, \\
t_3 &= \left(\frac{(\lambda_2-a_{11})\,a_{14}}{a_{12}\,(\lambda_2+1)} - \frac{b_{14}}{\lambda_2+1}\right) a_{12}\,(\lambda_2-a_{11})\,m_2 \\
&- \left(\frac{(\lambda_2-a_{11})\,a_{14}}{a_{12}\,(\lambda_2+1)} - \frac{b_{14}}{\lambda_2+1}\right) a_{12} m_2\,(1+a_{11}) \\
&- 2\left(\frac{(\lambda_2-a_{11})\,a_{15}}{a_{12}\,(\lambda_2+1)} - \frac{b_{15}}{\lambda_2+1}\right) (1+a_{11})\,(\lambda_2-a_{11})\,m_2 \\
&- \frac{(a_{11}-\lambda_2)\,e_2\,(\lambda_2-a_{11})\,m_1}{a_{12}\,(\lambda_2+1)} + \left(\frac{(\lambda_2-a_{11})\,e_1}{a_{12}\,(\lambda_2+1)} - \frac{e_3}{\lambda_2+1}\right) a_{12} m_1, \\
t_4 &= \left(\frac{(\lambda_2-a_{11})\,a_{14}}{a_{12}\,(\lambda_2+1)} - \frac{b_{14}}{\lambda_2+1}\right) a_{12}\,(\lambda_2-a_{11})\,m_3 \\
&- \left(\frac{(\lambda_2-a_{11})\,a_{14}}{a_{12}\,(\lambda_2+1)} - \frac{b_{14}}{\lambda_2+1}\right) a_{12} m_3\,(1+a_{11})
\end{aligned}
$$

$$
\begin{aligned}
&- \quad 2\left(\frac{(\lambda_2 - a_{11})\,a_{15}}{a_{12}\,(\lambda_2+1)} - \frac{b_{15}}{\lambda_2+1}\right)(1+a_{11})\,(\lambda_2 - a_{11})\,m_3 \\
&+ \quad \frac{(\lambda_2 - a_{11})^2\,e_2 m_2}{a_{12}\,(\lambda_2+1)} + \left(\frac{(\lambda_2 - a_{11})\,e_1}{a_{12}\,(\lambda_2+1)} - \frac{e_3}{\lambda_2+1}\right) a_{12} m_2, \\
t_5 \quad &= \quad \left(\frac{(\lambda_2 - a_{11})\,a_{13}}{a_{12}\,(\lambda_2+1)} - \frac{b_{13}}{\lambda_2+1}\right) a_{12}\,(1+a_{11})^2 \\
&+ \quad \left(\frac{(\lambda_2 - a_{11})\,a_{14}}{a_{12}\,(\lambda_2+1)} - \frac{b_{14}}{\lambda_2+1}\right) a_{12} m_1\,(\lambda_2 - a_{11}) \\
&+ \quad \left(\frac{(\lambda_2 - a_{11})\,a_{14}}{a_{12}\,(\lambda_2+1)} - \frac{b_{14}}{\lambda_2+1}\right) a_{12} m_1\,(1+a_{11}) \\
&- \quad 2\left(\frac{(\lambda_2 - a_{11})\,a_{15}}{a_{12}\,(\lambda_2+1)} - \frac{b_{15}}{\lambda_2+1}\right)(1+a_{11})\,(\lambda_2 - a_{11})\,m_1.
\end{aligned}
$$

Next, we have the coupled nonzero real numbers:

$$
\begin{aligned}
\digamma_1 \quad &= \quad \left(\frac{\partial^2 \tilde{f}}{\partial u \partial \bar{r}} + \frac{1}{2}\frac{\partial F}{\partial \bar{r}}\frac{\partial^2 F}{\partial u^2}\right)_{(0,0)} = \left(\frac{(\lambda_2 - a_{11})\,e_1}{a_{12}\,(\lambda_2+1)} - \frac{e_3}{\lambda_2+1}\right) a_{12} \\
&- \quad \frac{(\lambda_2 - a_{11})\,e_2\,(1+a_{11})}{a_{12}\,(\lambda_2+1)},
\end{aligned}
$$

and

$$
\digamma_2 \quad = \quad \left(\frac{1}{6}\frac{\partial^3 F}{\partial u^3} + \left(\frac{1}{2}\frac{\partial^2 F}{\partial u^2}\right)^2\right)_{(0,0)} = t_1^2 + t_5.
$$

We have the following conclusions according to aforemention calculation;

Theorem 2. *There exists flip bifurcation at* (x_*, y_*) *of (14) whenever* $\digamma_2 \neq 0$ *and* r *varies in small neighborhood of* r_1. *In addition, if* $\digamma_2 > 0$, $(\digamma_2 < 0)$ *respectively, then orbit having period-2 stable or unstable, respectively.*

Next, we investigate the Neimark-Sacker bifurcation of fixed point (x_*, y_*) of map (14). The main difference between Neimark-Sacker bifurcation of integer-order and fractional-order dynamical systems is that the fractional-order system can exhibit more complex and rich dynamics than the integer-order system, due to the presence of memory and hereditary effects in the fractional derivative term. For more recent work on bifurcation one can see [9–13, 28, 29, 40]. In order to explored the Neimark-Sacker bifurcation, we find the conditions for which (x_*, y_*) is non-hyperbolic point with complex conjugate root of characteristic equation of unit modulus. Thus if equation (16) hold true then $\mathbb{P}(\lambda) = 0$ have two complex conjugate root with unit modulus.

Consider,

$$T_{NS} = \{(\alpha, \rho, \mu, r) \in R_+^4 : (17)\ satisfied\}.$$

Assuming that
$r = r_2 = -\frac{2\mu^2\rho^\alpha + \sqrt{\Gamma(\alpha+1)((8\mu^2+1)\Gamma(\alpha+1) - 8\mu^2\rho^\alpha)} + (-2\mu^2-1)\Gamma(\alpha+1)}{2(\rho^\alpha - \Gamma(\alpha+1))}$, then fixed point (p_*, z_*) undergoes Neimark-Sacker bifurcation when parameters vary in the least neighborhood of T_{NS}. Thus system (14) along with parameters (α, ρ, μ, r_2) can be described by the following map:

$$\begin{pmatrix} x \\ y \end{pmatrix} \to \begin{pmatrix} x + \frac{\rho^\alpha}{\Gamma(\alpha+1)}\left[\mu - (r_2)x - xy^2\right] \\ y + \frac{\rho^\alpha}{\Gamma(\alpha+1)}\left[xy^2 - y + (r_2)x\right] \end{pmatrix}, \tag{23}$$

The following perturbation of system (23) can be obtained by taking $\tilde{r}$ as bifurcation parameter:

$$\begin{pmatrix} x \\ y \end{pmatrix} \to \begin{pmatrix} x + \frac{\rho^\alpha}{\Gamma(\alpha+1)}\left[\mu - (r_2+\tilde{r})x - xy^2\right] \\ y + \frac{\rho^\alpha}{\Gamma(\alpha+1)}\left[xy^2 - y + (r_2+\tilde{r})x\right] \end{pmatrix}. \tag{24}$$

where $|\tilde{r}| << 1$ is a least perturbation parameter.
Assuming that $H = x - x_*,\ P = y - y_*$, then system (24) is converted into the following form:

$$\begin{pmatrix} H \\ P \end{pmatrix} \to \begin{pmatrix} a_{11} & a_{12} \\ a_{21} & a_{22} \end{pmatrix}\begin{pmatrix} H \\ P \end{pmatrix} + \begin{pmatrix} \phi_1(H,P) \\ \phi_2(H,P) \end{pmatrix}, \tag{25}$$

where

$$\begin{aligned} \phi_1(H,P) &= a_{13}HP^2 + a_{14}HP + a_{15}P^2 + O\left((|H| + |P|)^4\right), \\ \phi_2(H,P) &= b_{13}HP^2 + b_{14}HP + b_{15}P^2 + O\left((|H| + |P|)^4\right). \end{aligned}$$

Where $a_{11}, a_{12},\ a_{21},\ a_{22}, a_{13},\ a_{14},\ a_{15},\ b_{13},\ b_{14},\ b_{15}$ are define in (20) by replacing r by $r_2 + \tilde{r}$. Let

$$\lambda^2 - A_1(\tilde{r})\lambda + A_2(\tilde{r}) = 0, \tag{26}$$

be the characteristics equation of variational matrix of system (25) evaluated at $(0,0)$, where $A_1(\tilde{r})$ and $A_2(\tilde{r})$ are defined in (25) with $r = r_2 + \tilde{r}$. Since $(\alpha, \rho, \mu, r_2) \in T_N S$, $|\lambda_1| = |\lambda_2|$ such that λ_1 and λ_2 are the complex conjugate root root of (26), then it follows that

$$\lambda_1, \lambda_2 = \frac{A_1(\tilde{r})}{2} \pm \frac{i}{2}\sqrt{4A_2(\tilde{r}) - A_1^2(\tilde{r})}.$$

Then we obtain

$$\begin{aligned}\left(\frac{d|\lambda_{1,2}|}{d\tilde{r}}\right)_{\tilde{r}=0} &= -\frac{\rho^\alpha\left(\sqrt{\Gamma(\alpha+1)\left(\left(8\mu^2+1\right)\Gamma(\alpha+1) - 8\mu^2\rho^\alpha\right)}\right)}{8\mu^2\Gamma(\alpha+1)^2} \\ &- \frac{\rho^\alpha\left(\left(8\mu^2+1\right)\Gamma(\alpha+1)\right)}{8\mu^2\Gamma(\alpha+1)^2} + \frac{\rho^\alpha\left(-8\mu^2\rho^\alpha\right)}{8\mu^2\Gamma(\alpha+1)^2} \neq 0\end{aligned}$$

Moreover $A_1(0) = 2 - \frac{\rho^\alpha\left(\mu^4+\mu^2(2r_2-1)+r_2(r_2+1)\right)}{\Gamma(\alpha+1)(\mu^2+2\mathrm{r}_{\_})} \neq 0,\ -1.$
Since, $(\alpha, \rho, \mu, r_2) \in T_{NS}$, it follows that
$-2 < A_1(0) = 2 - \frac{\rho^\alpha\left(\mu^4+\mu^2(2r_2-1)+r_2(r_2+1)\right)}{\Gamma(\alpha+1)(\mu^2+2\mathrm{r}_{\_})} < 2$. Thus we have $\lambda_1^m, \lambda_2^m \neq 1$ for all $m = 1, 2, 3, 4$ at $\tilde{r} = 0$, for $A_1(0) \neq 0, -1, \pm 2$. Hence, zeros of (26) do not lie in the intersection of the unit circle with the coordinate axes when $\tilde{r} = 0$.

The normal form of (25) at $\tilde{r} = 0$ can be obtained by taking $\theta = \frac{A_1(0)}{2}$, $\nu = \frac{1}{2}\sqrt{4A_2(0) - A_1^2(0)}$ and assuming the following transformation:

$$\begin{pmatrix} H \\ P \end{pmatrix} = \begin{pmatrix} a_{12} & 0 \\ \theta - a_{11} & -\nu \end{pmatrix} \begin{pmatrix} u \\ v \end{pmatrix}. \tag{27}$$

By using transformation (27), one has the following canonical form of system (25):

$$\begin{pmatrix} u \\ v \end{pmatrix} \rightarrow \begin{pmatrix} \theta & -\nu \\ \nu & \theta \end{pmatrix} \begin{pmatrix} u \\ v \end{pmatrix} + \begin{pmatrix} \widetilde{g_1}(u,v) \\ \widetilde{g_2}(u,v) \end{pmatrix}, \tag{28}$$

where

$$\begin{aligned} \widetilde{g_1}(u,v) &= \frac{a_{13}}{a_{12}} HP^2 + \frac{a_{14}}{a_{12}} HP + \frac{a_{15}}{a_{12}} P^2 + O\left((|u|+|v|)^4\right), \\ \widetilde{g_2}(u,v) &= \left(\frac{(a_{11}-\theta)\,a_{13}}{a_{12}\nu} + \frac{b_{13}}{\nu}\right) HP^2 + \left(\frac{(a_{11}-\theta)\,a_{14}}{a_{12}\nu} + \frac{b_{14}}{\nu}\right) HP \\ &+ \left(\frac{(\theta-a_{11})\,a_{15}}{a_{12}\nu} + \frac{b_{15}}{\nu}\right) P^2 + O\left((|u|+|v|)^4\right), \end{aligned}$$

where $H = a_{12}u$ and $P = (\theta - a_{11})u - \nu v$. Due to aforemention computation we state a non-zero real number:

$$\omega = \left(\left[-Re\left(\frac{(1-2\lambda_1)\lambda_2^2}{1-\lambda_1}\tau_{20}\tau_{11}\right) - \frac{1}{2}|\tau_{11}|^2 - |\tau_{02}|^2 + Re(\lambda_2\tau_{21})\right]\right)_{\tilde{r}=0},$$

where

$$\tau_{20} = \frac{1}{8}\left[\widetilde{g_1}_{uu} - \widetilde{g_1}_{vv} + 2\widetilde{g_2}_{uv} + i\left(\widetilde{g_2}_{uu} - \widetilde{g_2}_{vv} - 2\widetilde{g_1}_{uv}\right)\right],$$

$$\tau_{11} = \frac{1}{4}\left[\widetilde{g_1}_{uu} + \widetilde{g_1}_{vv} + i\left(\widetilde{g_2}_{uu} + \widetilde{g_2}_{vv}\right)\right],$$

$$\tau_{02} = \frac{1}{8}\left[\widetilde{g_1}_{uu} - \widetilde{g_1}_{vv} - 2\widetilde{g_2}_{uv} + i\left(\widetilde{g_2}_{uu} - \widetilde{g_2}_{vv} + 2\widetilde{g_1}_{uv}\right)\right],$$

$$\tau_{21} = \frac{1}{16}\left[\widetilde{g_1}_{uuu} + \widetilde{g_1}_{uvv} + \widetilde{g_2}_{uuv} + \widetilde{g_2}_{vvv} + i\left(\widetilde{g_2}_{uuu} + \widetilde{g_2}_{uvv} - \widetilde{g_1}_{uuv} - \widetilde{g_1}_{vvv}\right)\right].$$

We have the following conclusions for direction and existence of Neimark-Sacker bifurcation according to aforemention calculation;

Theorem 3. *There exists Neimark-Sacker bifurcation at* (x_*, y_*) *whenever* r *varies in a least neighborhood of* $r_2 = -\frac{2\mu^2\rho^\alpha + \sqrt{\Gamma(\alpha+1)((8\mu^2+1)\Gamma(\alpha+1)) - 8\mu^2\rho^\alpha} - (2\mu^2+1)\Gamma(\alpha+1)}{2(\rho^\alpha - \Gamma(\alpha+1))}$. *In addition, if* $\omega < 0, (\omega > 0)$, *respectively, then an attracting or repelling invariant closed curve bifurcates from the equilibrium point for* $r > r_2 (r < r_2)$, *respectively.*

4 Codimension-two bifurcations

This section deals with the study of codimension-two bifurcations. Particularly, we explore the existence of 1:2, 1:3 and 1:4 resonance by using normal form theory and theory of bifurcation. The occurrence of these resonances can be identified by the following curves:

$$R2: \frac{\rho^{\alpha}\left(\mu^4+\mu^2(2r-1)+r(r+1)\right)}{\Gamma(\alpha+1)\left(\mu^2+r\right)}=4,$$

$$R3: \frac{\rho^{\alpha}\left(\mu^4+\mu^2(2r-1)+r(r+1)\right)}{\Gamma(\alpha+1)\left(\mu^2+r\right)}=3,$$

$$R4: \frac{\rho^{\alpha}\left(\mu^4+\mu^2(2r-1)+r(r+1)\right)}{\Gamma(\alpha+1)\left(\mu^2+r\right)}=2,$$

and

$$NS: \frac{\rho^{\alpha}\left(\rho^{\alpha}\left(\mu^2+r\right)^2-\Gamma(\alpha+1)\left(\mu^4+\mu^2(2r-1)+r(r+1)\right)\right)}{\Gamma(\alpha+1)^2\left(\mu^2+r\right)}=0.$$

Then, it is easy to see that $R2\cap NS$, $R3\cap NS$ and $R4\cap NS$ are called 1:2 resonance point, 1:3 resonance point, and 1:4 resonance point, respectively. Furthermore, for $r\in[0,\ 5]$, $\mu\in[0,\ 5]$ and fixed $(\alpha,\ \rho)=(0.36,\ 0.672)$, the existence of strong resonance points of system (14) are depicted in Fig. 2.

4.1 1:2 strong resonance

In this subsection, we discuss 1:2 strong resonance for system (14) about its positive fixed point. For this, μ and r are taken as bifurcation parameters. The Jacobian matrix of the system (14) about positive fixed point has eigenvalue -1 with multiplicity two if the following conditions are satisfied:

$$\begin{cases} Tr: \frac{\rho^{\alpha}\left(\mu^4+\mu^2(2r-1)+r(r+1)\right)}{\Gamma(\alpha+1)(\mu^2+r)}=4 \\ Det: \frac{\rho^{\alpha}\left(\rho^{\alpha}\left(\mu^2+r\right)^2-\Gamma(\alpha+1)\left(\mu^4+\mu^2(2r-1)+r(r+1)\right)\right)}{\Gamma(\alpha+1)^2(\mu^2+r)}=0. \end{cases} \tag{29}$$

Solving system (29) for μ and r yields the following solution (μ_0, r_0):

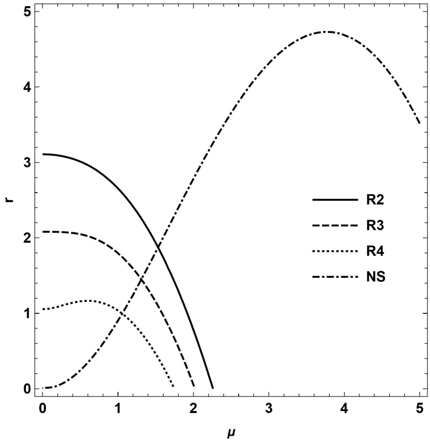

Figure 2. Existence of strong resonance points for system (14).

$$\mu_0 = -\sqrt{2}\rho^{-2\alpha}\Gamma(\alpha+1)\left(\rho^{\alpha} - 2\Gamma(\alpha+1)\right),$$

and

$$r_0 = 2\rho^{-4\alpha}\Gamma(\alpha+1)^2\left(\rho^{2\alpha} + 4\Gamma(\alpha+1)\left(\rho^{\alpha} - \Gamma(\alpha+1)\right)\right).$$

Taking the translations $u_n = x_n - x_*$, $v_n = y_n - y_*$, $\mu = \mu_0 + \bar{\mu}$ and $r = r_0 + \bar{r}$, then the system (14) can be transformed as follows:

$$\begin{pmatrix} u \\ v \end{pmatrix} \to \begin{pmatrix} 1+m_{11} & -m_{12} \\ m_{21} & 1+m_{22} \end{pmatrix}\begin{pmatrix} u \\ v \end{pmatrix} + \begin{pmatrix} f_1(u,v) \\ f_2(u,v,) \end{pmatrix}, \qquad (30)$$

where $\bar{\mu} << 1$ and $\bar{r} << 1$ are small perturbations,

$$\begin{aligned} f_1(u,v) &= m_{13}uv + m_{14}v^2 + O\left((|u|+|v|)^3\right), \\ f_2(u,v)) &= m_{23}uv + m_{24}v^2 + O\left((|u|+|v|)^3\right). \end{aligned}$$

$$m_{11}=-\frac{\rho^{\alpha}\left(\mu^{2}+r\right)}{\Gamma(\alpha+1)},\quad m_{12}=\frac{2\mu^{2}\rho^{\alpha}}{\Gamma(\alpha+1)\left(\mu^{2}+r\right)},\quad m_{21}=\frac{\rho^{\alpha}\left(\mu^{2}+r\right)}{\Gamma(\alpha+1)},$$

$$m_{22}=\frac{\rho^{\alpha}\left(\mu^{2}-r\right)}{\Gamma(\alpha+1)\left(\mu^{2}+r\right)},\quad m_{13}=-\frac{2\mu\rho^{\alpha}}{\Gamma(\alpha+1)},\quad m_{23}=\frac{2\mu\rho^{\alpha}}{\Gamma(\alpha+1)},$$

$$m_{14}=-\frac{\mu\rho^{\alpha}}{\Gamma(\alpha+1)\left(\mu^{2}+r\right)},\quad m_{24}=\frac{\mu\rho^{\alpha}}{\Gamma(\alpha+1)\left(\mu^{2}+r\right)}.$$

Next, we consider the following transformation:

$$\begin{pmatrix} u \\ v \end{pmatrix}=T\begin{pmatrix} w \\ z \end{pmatrix}, \tag{31}$$

where T is a nonsingular matrix given by

$$T=\begin{pmatrix} \frac{\mathrm{m12}}{\mathrm{m11+2}} & \frac{\mathrm{m12}}{(\mathrm{m11+2})^{2}} \\ 1 & 0 \end{pmatrix}.$$

From (30) and (31), it follows that:

$$\begin{pmatrix} w \\ z \end{pmatrix}\rightarrow\begin{pmatrix} p_{10}(\mu,r)-1 & p_{01}(\mu,r)+1 \\ q_{10}(\mu,r) & q_{01}(\mu,r)-1 \end{pmatrix}\begin{pmatrix} w \\ z \end{pmatrix}+\begin{pmatrix} f_{3}(w,z,\mu,r) \\ f_{4}(w,z,\mu,r) \end{pmatrix}, \tag{32}$$

where

$$f_{3}(w,z)=p_{20}w^{2}+p_{11}wz,\quad f_{4}(w,z)=q_{20}w^{2}+q_{11}wz,$$

$$p_{10}=2+\frac{m_{12}m_{21}}{2+m_{11}}+m_{22},\quad p_{01}=-1+\frac{m_{12}m_{21}}{(2+m_{11})^{2}},$$

$$q_{10}=-m_{12}m_{21}-2(2+m_{22})-m_{11}(2+m_{22}),\quad q_{01}=2+m_{11}-\frac{m_{12}m_{21}}{2+m_{11}},$$

$$p_{20} = \frac{m_{12}m_{23}}{2+m_{11}} + m_{24}, \quad p_{11} = \frac{m_{12}m_{23}}{(2+m_{11})^2},$$

$$q_{20} = \frac{m_{14}\,(m_{11}+2)^{\,2} + m_{12}\,(m_{13}-m_{24})\,(m_{11}+2) - m_{12}^2 m_{23}}{m_{12}},$$

$$q_{11} = m_{13} - \frac{m_{12}m_{23}}{m_{11}+2}.$$

Next, we consider the following invertible linear transformation:

$$\begin{pmatrix} w \\ z \end{pmatrix} = M \begin{pmatrix} \bar{w} \\ \bar{z} \end{pmatrix}, \tag{33}$$

where

$$M = \begin{pmatrix} 1+p_{01}(\mu,r) & 0 \\ -p_{01}(\mu,r) & 1 \end{pmatrix}.$$

From (32) and (34), it follows that:

$$\begin{pmatrix} \bar{w} \\ \bar{z} \end{pmatrix} \to \begin{pmatrix} -1 & 1 \\ \theta_1(\mu,r) & \theta_1(\mu,r)-1 \end{pmatrix} \begin{pmatrix} \bar{w} \\ \bar{z} \end{pmatrix} + \begin{pmatrix} f_5(\bar{w},\bar{z},\mu,r) \\ f_6(\bar{w},\bar{z},\mu,r) \end{pmatrix}, \tag{34}$$

where

$$\theta_1(\mu,r) = q_{10} + p_{01}q_{10} - p_{10}q_{01}, \quad \theta_2(\mu,r) = p_{10} + q_{01} - 1$$

$$f_5(\bar{w},\bar{z},\mu,r) = \bar{p}_{20}\bar{w}^2 + \bar{p}_{11}\bar{w}\bar{z}, \quad f_6(\bar{w},\bar{z},\mu,r) = \bar{q}_{20}\bar{w}^2 + \bar{q}_{11}\bar{w}\bar{z},$$

$$\bar{p}_{20} = p_{20} + p_{01}p_{20} - p_{10}p_{11}, \quad \bar{p}_{11} = p_{11}, \quad \bar{q}_{11} = p_{10}p_{11} + q_{11} + p_{01}q_{11}$$

$$\bar{q}_{20} = (1+p_{01})p_{10}(p_{20}-q_{11}) + (1+p_{01})^2 q_{20} - p_{10}^2 p_{11}.$$

Taking into account θ_1 and θ_2, we define the following matrix:

$$\mathbb{S}(\mu_0, r_0) = \begin{pmatrix} \frac{\partial\theta_1}{\partial\mu}(\mu_0, r_0) & \frac{\partial\theta_1}{\partial r}(\mu_0, r_0) \\ \frac{\partial\theta_2}{\partial\mu}(\mu_0, r_0) & \frac{\partial\theta_2}{\partial r}(\mu_0, r_0) \end{pmatrix}.$$

Then by simple computation $det\mathbb{S}(\mu_0, r_0)$ is computed as follows:

$$det\mathbb{S}(\mu_0, r_0) = \frac{4\mu\rho^{2\alpha}\left(\rho^\alpha - \Gamma(\alpha+1)\right)}{\Gamma(\alpha+1)^3\left(\mu^2+r\right)} \neq 0 \tag{35}$$

Condition (35) is called transversality assumption, and we assume that it holds true. Next, $\theta_1(\mu, r)$ and $\theta_2(\mu, r)$ can be used for the following parametrization in the neighborhood of $\mu = \mu_0$ and $r = r_0$:

$$\beta_1 = \theta_1(\mu, r), \quad \beta_2 = \theta_2(\mu, r).$$

Then, μ and r can be expressed in terms of β_1 and β_2 as follows:

$$\begin{cases} \mu = \frac{\rho^{-\alpha}\Gamma(\alpha+1)\sqrt{\frac{\beta 1}{2}+\beta 2-2}}{\sqrt{(\rho^\alpha-\Gamma(\alpha+1))^2}} \\ \times\left(\sqrt{\Gamma(\alpha+1)^2(\beta 1+3\beta 2-9)-(\beta 2-6)\rho^\alpha\Gamma(\alpha+1)-\rho^{2\alpha}}\right), \end{cases} \tag{36}$$

and

$$\begin{cases} r = -\frac{\left(\Gamma(\alpha+1)^2(\beta 1+3\beta 2-9)-(\beta 2-4)\rho^\alpha\Gamma(\alpha+1)+\rho^{2\alpha}\right)}{2(\rho^\alpha-\Gamma(\alpha+1))^2} \\ \times\left(\rho^{-2\alpha}\Gamma(\alpha+1)^2(\beta 1+2\beta 2-4)\right). \end{cases} \tag{37}$$

Using (36) and (37) in (34), we have the following mapping:

$$\begin{pmatrix} \bar{w} \\ \bar{z} \end{pmatrix} \to \begin{pmatrix} -1 & 1 \\ \beta_1 & -1+\beta_2 \end{pmatrix} \begin{pmatrix} \bar{w} \\ \bar{z} \end{pmatrix} + \begin{pmatrix} f_7(\bar{w}, \bar{z}, \beta_1, \beta_2) \\ f_8(\bar{w}, \bar{z}, \beta_1, \beta_2) \end{pmatrix}, \tag{38}$$

where

$$f_7(\bar{w}, \bar{z}, \beta_1, \beta_2) = g_{20}\bar{w}^2(\beta_1, \beta_2) + g_{11}\bar{w}\bar{z}(\beta_1, \beta_2),$$

$$f_8(\bar{w}, \bar{z}, \beta_1, \beta_2) = h_{20}\bar{w}^2(\beta_1, \beta_2) + h_{11}\bar{w}\bar{z}(\beta_1, \beta_2),$$

$h_{20} = \frac{(m_{12}(m_{14}m_{21}^2 - m_{13}m_{21}(2+m_{22}) + (2+m_{22})(-(2+m_{22})m_{23} + m_{21}m_{24})))}{(2+m_{11})^2}$,

$$\begin{aligned} g_{20}(\beta_1,\beta_2) &= \frac{m_{12}\left(m_{21}m_{24} - \left(m_{22}+2\right)m_{23}\right)}{\left(m_{11}+2\right)^2}, \\ g_{11}(\beta_1,\beta_2) &= \frac{m_{12}m_{23}}{\left(m_{11}+2\right)^2}, \\ h_{11}(\beta_1,\beta_2) &= \frac{m_{12}\left(m_{13}m_{21} + \left(m_{22}+2\right)m_{23}\right)}{\left(2+m_{11}\right)^2}. \end{aligned}$$

Then according to Lemma 9.9 [[42], p. 437], there exists a nearidentity transformation such that system (34) can be transformed as follows:

$$\begin{pmatrix} x_1 \\ x_2 \end{pmatrix} \to \begin{pmatrix} -1 & 1 \\ \beta_1 & -1+\beta_2 \end{pmatrix} \begin{pmatrix} x_1 \\ x_2 \end{pmatrix} + \begin{pmatrix} 0 \\ Cx_1^3 + Dx_1x_2 \end{pmatrix} \quad (39)$$
$$+ O(|x_1 + x_2|^4),$$

where

$$C(\beta_1,\beta_2) = g_{20}(\beta_1,\beta_2)h_{20}(\beta_1,\beta_2) + \frac{1}{2}h_{20}^2(\beta_1,\beta_2) + \frac{1}{2}h_{20}(\beta_1,\beta_2)h_{11}(\beta_1,\beta_2),$$

$$\begin{aligned} D(\beta_1,\beta_2) &= \frac{1}{2}g_{20}(\beta_1,\beta_2)h_{11}(\beta_1,\beta_2) + \frac{5}{4}h_{20}(\beta_1,\beta_2)h_{11}(\beta_1,\beta_2) \\ &+ h_{20}^2(\beta_1,\beta_2) + \frac{1}{2}h_{11}^2(\beta_1,\beta_2) + h_{20}(\beta_1,\beta_2)h_{02}(\beta_1,\beta_2) \\ &+ 3g_{20}^2(\beta_1,\beta_2) + \frac{5}{2}g_{20}(\beta_1,\beta_2)h_{20}(\beta_1,\beta_2) \\ &+ \frac{5}{2}g_{11}(\beta_1,\beta_2)h_{20}(\beta_1,\beta_2). \end{aligned}$$

Lastly, simple computation yields that

$$C(0,0) = \frac{\left(\rho^\alpha - 3\Gamma(\alpha+1)\right)^2\left(\rho^{2\alpha} + 3\Gamma(\alpha+1)\left(\rho^\alpha - 4\Gamma(\alpha+1)\right)\right)}{2\Gamma(\alpha+1)^3\left(\rho^\alpha - \Gamma(\alpha+1)\right)},$$

$$D(0,0) = 106 - \frac{33\rho^{2\alpha}}{4\Gamma(\alpha+1)^2} + \frac{\rho^{3\alpha}}{4\Gamma(\alpha+1)^3} + \frac{\rho^{4\alpha}}{4\Gamma(\alpha+1)^4}$$

$$+ \quad \frac{64\Gamma(\alpha+1)^2}{(\rho^\alpha - \Gamma(\alpha+1))^2} - \frac{9\rho^\alpha}{4\Gamma(\alpha+1)} - \frac{136\Gamma(\alpha+1)}{\rho^\alpha - \Gamma(\alpha+1)}.$$

Taking into account above calculation and theoretical results presented in [42], we have the following result.

Theorem 4. *Assume that $C(0,0) \neq 0$, $D(0,0) + 3C(0,0) \neq 0$, and $det\mathbb{S}(\mu_0, r_0) \neq 0$ then system (14) undergoes 1:2 strong resonance about its positive fixed point whenever μ and r vary in small neighborhoods of μ_0 and r_0, respectively.*

4.2 1:3 strong resonance

In this section, we discuss 1:3 strong resonance for system (14) about its positive fixed point. For this, μ and r are taken as bifurcation parameters. Then Jacobian matrix of the system (14) about positive fixed point has complex conjugate eigenvalue $-\frac{1}{2} \pm \iota\frac{\sqrt{3}}{2}$ if the following conditions are satisfied:

$$\begin{cases} Tr : \frac{\rho^\alpha\left(\mu^4+\mu^2(2r-1)+r(r+1)\right)}{\Gamma(\alpha+1)(\mu^2+r)} = 3 \\ Det : \frac{\rho^\alpha\left(\rho^\alpha\left(\mu^2+r\right)^2-\Gamma(\alpha+1)\left(\mu^4+\mu^2(2r-1)+r(r+1)\right)\right)}{\Gamma(\alpha+1)^2(\mu^2+r)} = 0. \end{cases} \tag{40}$$

Solving system (40) for μ and r yields the following solution (μ_1, r_1):

$$\mu_1 = \sqrt{\frac{3}{2}}\sqrt{\rho^{-4\alpha}\Gamma(\alpha+1)^2\left(\rho^{2\alpha} - 3\rho^\alpha\Gamma(\alpha+1) + 3\Gamma(\alpha+1)^2\right)},$$

$$r_1 = \frac{3}{2}\rho^{-4\alpha}\Gamma(\alpha+1)^2\left(\rho^{2\alpha} + 3\Gamma(\alpha+1)\left(\rho^\alpha - \Gamma(\alpha+1)\right)\right).$$

In order to shift the positive fixed point (x_*, y_*) of (14) at $(0,0)$, the translation $u_n = x_n - x_*$, $v_n = y_n - y_*$ and $\mu = \mu_1$ and $r = r_1$ yields the following system then system (14) can be described by the following map:

$$\begin{pmatrix} u \\ v \end{pmatrix} \to \begin{pmatrix} \epsilon_{11} & \epsilon_{12} \\ \epsilon_{21} & \epsilon_{22} \end{pmatrix}\begin{pmatrix} u \\ v \end{pmatrix} + \begin{pmatrix} f_1(u,v) \\ f_2(u,v,) \end{pmatrix}, \tag{41}$$

$$\begin{aligned}\epsilon_{11} &= 1-3\rho^{-\alpha}\Gamma(\alpha+1), \quad \epsilon_{12}=-3\rho^{-\alpha}\Gamma(\alpha+1)-\frac{\rho^{\alpha}}{\Gamma(\alpha+1)}+3,\\ \epsilon_{21} &+ 3\rho^{-\alpha}\Gamma(\alpha+1), \quad \epsilon_{22}=3\rho^{-\alpha}\Gamma(\alpha+1)-2,\end{aligned}$$

$$\begin{aligned} f_1(u,v) &= a_{11}uv+a_{02}v^2+O\left((|u|+|v|)^3\right),\\ f_2(u,v)) &= b_{11}uv+b_{02}v^2+O\left((|u|+|v|)^3\right).\end{aligned}$$

$$a_{02}=-\frac{\rho^{3\alpha}\sqrt{\rho^{-4\alpha}\Gamma(\alpha+1)^2\left(\rho^{2\alpha}-3\rho^{\alpha}\Gamma(\alpha+1)+3\Gamma(\alpha+1)^2\right)}}{\sqrt{6}\Gamma(\alpha+1)^3},$$

$$a_{11}=-\frac{\sqrt{6}\rho^{\alpha}\sqrt{\rho^{-4\alpha}\Gamma(\alpha+1)^2\left(\rho^{2\alpha}-3\rho^{\alpha}\Gamma(\alpha+1)+3\Gamma(\alpha+1)^2\right)}}{\Gamma(\alpha+1)},$$

$$b_{02}=\frac{\rho^{3\alpha}\sqrt{\rho^{-4\alpha}\Gamma(\alpha+1)^2\left(\rho^{2\alpha}-3\rho^{\alpha}\Gamma(\alpha+1)+3\Gamma(\alpha+1)^2\right)}}{\sqrt{6}\Gamma(\alpha+1)^3},$$

$$b_{11}=\frac{\sqrt{6}\rho^{\alpha}\sqrt{\rho^{-4\alpha}\Gamma(\alpha+1)^2\left(\rho^{2\alpha}-3\rho^{\alpha}\Gamma(\alpha+1)+3\Gamma(\alpha+1)^2\right)}}{\Gamma(\alpha+1)}.$$

The eigenvalues of jacobian matrix of system (41) are $\frac{-1}{2}\pm\frac{\sqrt{3}}{2}\iota$, let $p_1(\mu_1,r_1)$ and $q_1(\mu_1,r_1)$ are eigenvector associated with jacobian matrix of (41) and its transpose, respectively and satisfying $\langle p_1(\mu_1,r_1),q_1(\mu_1,r_1)\rangle=1$. Then, by simple computation one has;

$$p_1(\mu_1,r_1)=\begin{pmatrix}\frac{\left(3+i\sqrt{3}\right)\rho^{\alpha}}{6\Gamma(\alpha+1)}-1\\ 1\end{pmatrix},$$

and

$$q_1(\mu_1,r_1)=\begin{pmatrix}\frac{6(-1)^{2/3}\Gamma(\alpha+1)}{\left(3-i\sqrt{3}\right)\rho^{\alpha}+3\left(i+\sqrt{3}\right)i\Gamma(\alpha+1)}\\ 1\end{pmatrix}.$$

Moreover, any $X \in \mathbb{R}^2$ can be described uniquely as follows:

$$X = zp_1(\mu_1, r_1) + \bar{z}\bar{p_1}(\mu_1, r_1), \quad z \in \mathcal{C}.$$

Consequently, the complex form for the map (41) can be written as follows:

$$z \longrightarrow \left(\frac{-1}{2} + \frac{\sqrt{3}}{2}\iota \right) z + \sum_{2 \le j+k \le 3} \frac{1}{j!k!} g_{jk} z^j \bar{z}^k, \tag{42}$$

where

$$g_{20} = -2i\sqrt{3}\rho^{-\alpha}\Gamma(\alpha+1)(a_{02} - a_{11} + b_{02}) - i\sqrt{3}a_{11} + a_{11} + b_{02} + \sqrt{3}ib_{02},$$

$$g_{11} = 2\sqrt{3}i\rho^{-\alpha}\Gamma(\alpha+1)(a_{11} - b_{02} - a_{02}) + \sqrt{3}ib_{02}b_{02} - i\sqrt{3}a_{11},$$

$$g_{02} = 2i\sqrt{3}\rho^{-\alpha}\Gamma(\alpha+1)(a_{11} - b_{02} - a_{02}) - i\left(\sqrt{3} - i\right)(a_{11} - b_{02})$$

and $g_{30} = g_{03} = g_{12} = g_{21} = 0$.

Next, according to Lemma 9.12 [[42], p. 448], there exists a smoothly parameter dependent change of variable such that the map (42) can be converted into the following form:

$$w \longrightarrow \left(\frac{-1}{2} + \frac{\sqrt{3}}{2}\iota \right) w + B(\mu_1, r_1)\bar{w} + C(\mu_1, r_1)w|w|^2 + \left(|w|^4\right), \tag{43}$$

where

$$B(\mu_1, r_1) = \frac{1}{2}g_{02},$$

and

$$C(\mu_1, r_1) = \left(\frac{1}{2} + \frac{\sqrt{3}}{2}\iota \right) g_{02}g_{11} + \left(\frac{2}{2} + \frac{-1}{2\sqrt{3}}\iota \right) |g_{11}| .$$

Next, we consider the following quantities:

$$B_1(\mu,r_1) = \left(\frac{-3}{2} + \frac{3\sqrt{3}}{2}\iota \right) B(\mu_1, r_1)$$

$$C_1(\mu_1, r_1) = -3\left|B(\mu_1, r_1)\right|^2 - \frac{3}{2}(1+\sqrt{3}\iota)C(\mu_1, r_1).$$

Arguing as in Lemma 9.13 [[42], p. 450], we have the following result.

Theorem 5. *Assume that $\mu = \mu_1$, $r = r_1$, $ReC_1(\mu_1, r_1) \neq 0$ and $B(\mu_1, r_1)$ $\neq 0$ then the system (14) undergoes a 1:3 resonance about its positive fixed point, $ReC_1(\mu_1, r_1) \neq 0$ determines the stability nature for the bifurcating closed invariant curve.*

4.3 1:4 strong resonance

In this section, we discuss 1:4 strong resonance for system (14) about its positive fixed point. For this, μ and r are taken as bifurcation parameters. Then Jacobian matrix of the system (14) about positive fixed point has complex conjugate eigenvalue$\pm\iota$ if the following conditions are satisfied:

$$\begin{cases} Tr : \frac{\rho^\alpha\left(\mu^4+\mu^2(2r-1)+r(r+1)\right)}{\Gamma(\alpha+1)(\mu^2+r)} = 2 \\ Det : \frac{\rho^\alpha\left(\rho^\alpha\left(\mu^2+r\right)^2-\Gamma(\alpha+1)\left(\mu^4+\mu^2(2r-1)+r(r+1)\right)\right)}{\Gamma(\alpha+1)^2(\mu^2+r)} = 0. \end{cases} \tag{44}$$

Solving system (44) for μ and r yields the following solution (μ_2, r_2):

$$\mu_2 = \rho^{-2\alpha}\Gamma(\alpha+1)\sqrt{\rho^{2\alpha} - 2\rho^\alpha\Gamma(\alpha+1) + 2\Gamma(\alpha+1)^2},$$

$$r_2 = \rho^{-4\alpha}\Gamma(\alpha+1)^2\left(\rho^{2\alpha} + 2\Gamma(\alpha+1)\left(\rho^\alpha - \Gamma(\alpha+1)\right)\right).$$

In order to shift the positive fixed point (x_*, y_*) of (14) at $(0,0)$, the translation $u_n = x_n - x_*$, $v_n = y_n - y_*$ and $\mu = \mu_2$ and $r = r_2$ yields the following system then system (14) can be described by the following map:

$$\begin{pmatrix} u \\ v \end{pmatrix} \to \begin{pmatrix} \varepsilon_{11} & \varepsilon_{12} \\ \varepsilon_{21} & \varepsilon_{22} \end{pmatrix} \begin{pmatrix} u \\ v \end{pmatrix} + \begin{pmatrix} f_1(u,v) \\ f_2(u,v,) \end{pmatrix}, \tag{45}$$

$$\begin{aligned}\varepsilon_{11} &= 1-2\rho^{-\alpha}\Gamma(\alpha+1), \quad \varepsilon_{12}=-2\rho^{-\alpha}\Gamma(\alpha+1)-\frac{\rho^{\alpha}}{\Gamma(\alpha+1)}+2,\\ \varepsilon_{21} &= 2\rho^{-\alpha}\Gamma(\alpha+1), \quad \varepsilon_{22}=2\rho^{-\alpha}\Gamma(\alpha+1)-1,\end{aligned}$$

$$\begin{aligned}f_1(u,v) &= a_{11}uv+a_{02}v^2+O\left((|u|+|v|)^3\right),\\ f_2(u,v)) &= b_{11}uv+b_{02}v^2+O\left((|u|+|v|)^3\right).\end{aligned}$$

$$a_{02}=-\frac{\rho^{\alpha}\sqrt{\rho^{2\alpha}-2\rho^{\alpha}\Gamma(\alpha+1)+2\Gamma(\alpha+1)^2}}{2\Gamma(\alpha+1)^2},$$

$$a_{11}=-2\rho^{-\alpha}\sqrt{\rho^{2\alpha}-2\rho^{\alpha}\Gamma(\alpha+1)+2\Gamma(\alpha+1)^2},$$

$$b_{02}=\frac{\rho^{\alpha}\sqrt{\rho^{2\alpha}-2\rho^{\alpha}\Gamma(\alpha+1)+2\Gamma(\alpha+1)^2}}{2\Gamma(\alpha+1)^2},$$

$$b_{11}=2\rho^{-\alpha}\sqrt{\rho^{2\alpha}-2\rho^{\alpha}\Gamma(\alpha+1)+2\Gamma(\alpha+1)^2}.$$

The eigenvalues of jacobian matrix of system (45) are $\pm\iota$, let $p_2(\mu_2,r_2)$ and $q_2(\mu_2,r_2)$ are eigenvector associated with jacobian matrix of (45) and its transpose, respectively and satisfying $\langle p_2(\mu_2,r_2), q_2(\mu_2,r_2)\rangle = 1$. Then, by simple computation one has;

$$p_2(\mu_2,r_2)=\begin{pmatrix}\frac{\left(\frac{1}{2}-\frac{i}{2}\right)\rho^{\alpha}}{\Gamma(\alpha+1)}-1\\ 1\end{pmatrix},$$

and

$$q_2(\mu_2,r_2)=\begin{pmatrix}\frac{1}{1-\frac{\left(\frac{1}{2}-\frac{i}{2}\right)\rho^{\alpha}}{\Gamma(\alpha+1)}}\\ 1\end{pmatrix}.$$

Moreover, any $X\in\mathbb{R}^2$ can be described uniquely as follows:

$$X=zp_2(\mu_2,r_2)+\bar{z}\bar{p_2}(\mu_2,r_2), \quad z\in\mathcal{C}.$$

Consequently, the complex form for the map (45) can be written as follows:

$$z \longrightarrow (\iota)\, z + \sum_{2 \le j+k \le 3} \frac{1}{j!k!} \bar{g}_{jk} z^j \bar{z}^k, \tag{46}$$

where

$$\bar{g}_{20} = \left(\frac{1}{2} + \frac{i}{2}\right)(a_{11} - ib_{02}) - i\rho^{-\alpha}\Gamma(\alpha+1)(a_{11} - b_{02} - a_{02}),$$

$$\bar{g}_{11} = i(a_{11} - (1+i)b_{02}) - 2i\rho^{-\alpha}\Gamma(\alpha+1)(a_{11} - b_{02} - a_{02}),$$

$$\bar{g}_{02} = \left(-\frac{1}{2} + \frac{i}{2}\right)(a_{11} - b_{02}) - i\rho^{-\alpha}\Gamma(\alpha+1)(a_{11} - b_{02} - a_{02}),$$

and $\bar{g}_{30} = \bar{g}_{03} = \bar{g}_{12} = \bar{g}_{21} = 0$.

Next, according to Lemma 9.13 [[42], p. 448], there exists a smoothly parameter dependent change of variable such that the map (46) can be converted into the following form:

$$w_1 \longrightarrow (\iota)\, w_1 + B_1(\mu_2, r_2) w_1 |w_1|^2 + C_1(\mu_2, r_2) w_1^3 + \left(|w_1|^4\right), \tag{47}$$

where

$$B_1(\mu_2, r_2) = \iota \bar{g}_{11} - \frac{1}{2}\bar{g}_{11}\bar{\bar{g}}_{20}(1+\iota) + \bar{\bar{g}}_{11}\bar{g}_{20} + \bar{g}_{02}\bar{g}_{11}(\iota - 1) - \frac{1}{2}\bar{g}_{11}\bar{g}_{20}(1 - 2\iota),$$

and

$$C_1(\mu_2, r_2) = \frac{\iota - 1}{4}\bar{g}_{11}\bar{g}_{02} - \frac{\iota + 1}{4}\bar{g}_{11}\bar{g}_{20}.$$

Next, we consider the following quantities:

$$B_2(\mu_2, r_2) = -4\iota B_1(\mu_2, r_2)$$

$$C_2(\mu_2, r_2) = -4\iota C_1(\mu_2, r_2),$$

whenever $C_2(\mu_1, r_1) \neq 0$, thus we can write jacobian matrix $J(\mu_2, r_2) = \frac{B_2(\mu_2, r_2)}{|C_2(\mu_2, r_2)|}$. Arguing as in Lemma 9.15 [[42], p. 450], we have the following result.

Theorem 6. *Assume that* $\mu = \mu_2$*,* $r = r_2$*,* $ReJ(\mu_2, r_2) \neq 0$ *and* $ImJ(\mu_2, r_2) \neq 0$ *then the system (14) undergoes a 1:4 resonance about its positive fixed point,* $ReJ(\mu_2, r_2) \neq 0$ *determines the stability nature for the bifurcating closed invariant curve.*

5 Numerical simulation

This section aims to validate the theoretical analysis presented earlier by demonstrating the dynamic and chaotic behavior of the system (14) with selected parameter values. Our focus is primarily on the stability analysis and bifurcation behavior of the system's positive equilibrium. To accomplish this, we employ various mathematical tools such as Mathematica packages to generate plots, phase portraits, bifurcation diagrams and maximum Lyapunov characteristic exponents associated with the system (14). Initially, to observe the qualitative changes due to bifurca-

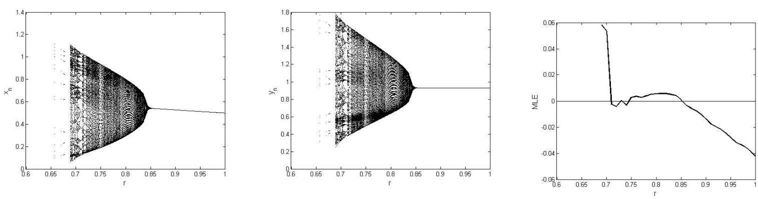

(a) Bifurcation diagram for x_n **(b)** Bifurcation diagram for y_n **(c)** MLE

Figure 3. MLE and Bifurcation diagrams for system (14) with $(\rho,\ \alpha,\ \mu) = (0.34, 0.01, 0.93)$, $r \in [0.6,\ 1]$ and initial conditions $(x_0,\ y_0) = (0.5, 0.9)$

tion we take $(\rho,\ \alpha,\ \mu) = (0.34, 0.01, 0.93)$. Let $r \in [0.6,\ 1]$ be the bifurcation parameter, then system (14) undergoes hopf bifurcation at

$r_1 = 0.8499470761490069$. For these parametric values, the positive fixed point is $(x_*,\ y_*) = (0.542322,\ 0.93)$. The eigenvalues of Jacobian matrix of system (14) about $(x_*,\ y_*) = (0.542322,\ 0.93)$ are $\lambda_{1,\ 2} = 0.151274 \pm 0.988492\iota$ and $|\lambda_{1,\ 2}| = 1$. Alternatively,the bifurcation diagrams for for system (14) in (r, x_n) and (r, y_n) planes are depicted in Fig. 3a and Fig. 3b, respectively and crossposting MLE are directed in Fig. 3c. Moreover, to explore the complex behavior of system (14), some phase portraits are presented in Fig. 4a, Fig. 4b, Fig. 4c, Fig. 4d

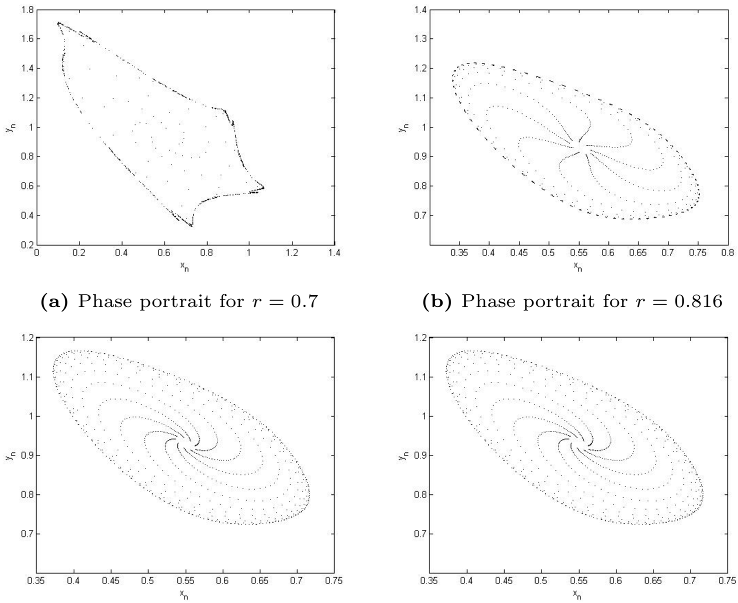

(a) Phase portrait for $r = 0.7$ **(b)** Phase portrait for $r = 0.816$

(c) Phase portrait for $r = 0.826$ **(d)** Phase portrait for $r = 0.836$

Figure 4. Phase portrait for system (14)

Next, assume $(\rho,\ \alpha,\ \mu) = (0.18,\ 0.34,\ 1.4)$ and $r \in [2.2,\ 2.6]$ be a bifurcation parameter, then system (14) undergoes flip bifurcation about $r_2 = 5.63587348174116$. In this case unique positive equilibrium point of system (14) is $(x_*,\ y_*) = (0.184311,\ 1.4)$. Moreover, eigenvalues of Jacobian matrix of system (14) are $\lambda_1 = -1$ and $|\lambda_2| = 0.689406 \neq \pm 1$. Alternatively, the bifurcation diagrams for for system (14) in (r, x_n) and (r, y_n) planes are depicted in Fig. 5a and Fig. 5b, respectively and crossposting MLE are directed in Fig. 5c.

Next, assume $(\rho,\ \alpha) = (0.18,\ 0.34)$, $r \in [1.16,\ 1.24]$ and $\mu \in [1.93,\ 1.96]$. Let $(r_0, \mu_0) = (1.142316212430117,\ 1.972448414307462)$ be the bifurcation parameters, then system (14) undergoes 1:2 resonance about unique positive fixed point $(x_*,\ y_*) = (0.391913,\ 1.97245)$. Moreover, eigenvalues of Jacobian matrix of system (14) are $\lambda_{1,2} \equiv -1$. Alternatively, the bifurcation diagrams and crossposting MLE for for system (14) in $(r,\ \mu,\ x_n)$ and $(r,\ \mu,\ y_n)$ spaces are depicted in Fig. 6a, Fig. 6b and, Fig. 6c, respectively.

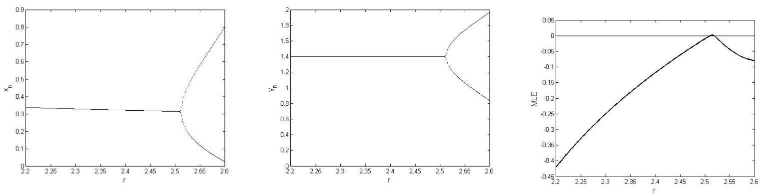

(a) Bifurcation diagram for x_n **(b)** Bifurcation diagram for y_n **(c)** MLE

Figure 5. MLE and Bifurcation diagrams for system (14) with $(\rho,\ \alpha,\ \mu) = (0.18,\ 0.34,\ 1.4)$, $r \in [2.2,\ 2.6]$ and initial conditions $(x_0,\ y_0) = (0.18,\ 1, 4)$

Next, assume $(\rho,\ \alpha) = (0.741,\ 0.846)$, $r \in [1.419, 1.8]$ and $\mu \in [1.343, 1.345]$. Let $(r_0, \mu_0) = (1.424848274436868,\ 1.3444958506301898)$ be the bifurcation parameters, then system (14) undergoes 1:3 resonance about unique positive fixed point $(x_*,\ y_*) = (0.41592842298066773, 1.3444958506301898)$. Moreover, eigenvalues of Jacobian matrix of system (14) are $\lambda_{1,2} = \frac{-1+\sqrt{3}\iota}{2}$. Alternatively, the bifurcation diagrams and corresponding MLE for for system (14) in $(r,\ \mu,\ x_n)$ and $(r,\ \mu,\ y_n)$ spaces are depicted in Fig. 7a, Fig. 7b and Fig. 7c, respectively.

Next, assume $(\rho,\ \alpha) = (0.85,\ 0.95)$, $r \in [0.95, 1.5]$ and $\mu \in [0.9, 1]$. Let $(r_0, \mu_0) = (0.9992608065977496,\ 0.9757272955467994)$ be the bifurcation parameters, then system (14) undergoes 1:3 resonance about unique positive fixed point $(x_*,\ y_*) = (0.5000384433121589,\ 0.9757272955467994)$. Alternatively, the bifurcation diagrams and crossposting MLE for for system (14) in $(r,\ \mu,\ x_n)$ and $(r,\ \mu,\ y_n)$ spaces are depicted in Fig. 8a, Fig. 8b and Fig. 8c, respectively.

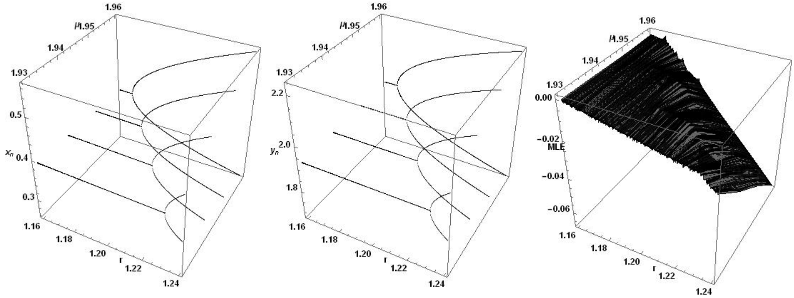

(a) Bifurcation diagram for x_n **(b)** Bifurcation diagram for y_n **(c)** MLE

Figure 6. MLE and Bifurcation diagrams for system (14) with $(\rho,\ \alpha) = (0.18,\ 0.34)$, $r \in [1.16,\ 1.24]$, $\mu \in [1.93,\ 1.96]$ and initial conditions $(x_0,\ y_0) = (0.39,\ 1.97)$

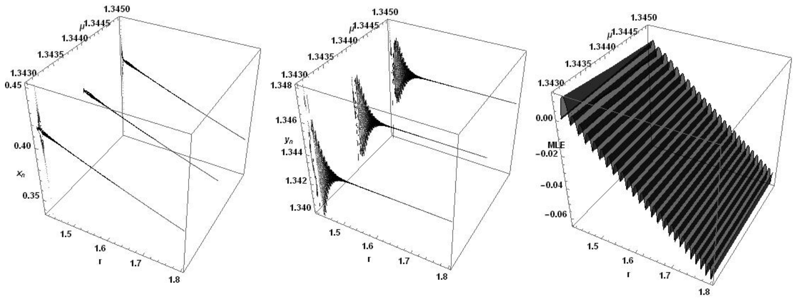

(a) Bifurcation diagram for x_n **(b)** Bifurcation diagram for y_n **(c)** MLE

Figure 7. MLE and Bifurcation diagrams for system (14) with $(\rho,\ \alpha) = (0.741, 0.846)$, $r \in [1.419, 1.8]$, $\mu \in [1.343, 1.345]$ and initial conditions $(x_0,\ y_0) = (0.415928,\ 1.3445)$

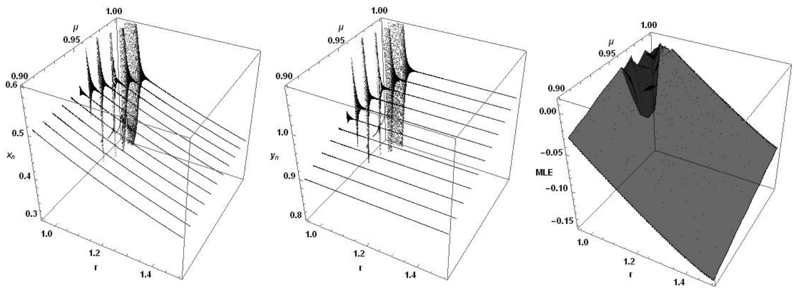

(a) Bifurcation diagram for x_n **(b)** Bifurcation diagram for y_n **(c)** MLE

Figure 8. MLE and Bifurcation diagrams for system (14) with $(\rho,\ \alpha) = (0.95, 0.85)$, $r \in [0.95, 1.5]$, $\mu \in [0.9, 1]$ and initial conditions $(x_0,\ y_0) = (0.5,\ 0.975727)$

6 Conclusion

A chemical reaction model is considered for its discritization and qualitative analysis. By applying the Caputo fractional derivative the discrete-time fractional order cubic autocatalator chemical reaction model is obtained. It is proved that system has a unique positive equilibrium point. The local dynamical behavior of model is studied. Particularly, parametric conditions are obtained for local asymptotic stability of model (14). Furthermore, codimension-one and codimension-two bifurcations are discussed. By implementing normal form method and bifurcation theory, it is proved that system (14) undergoes Neimark-Sacker bifurcation and period-doubling bifurcation at its positive equilibrium point. Moreover, it is shown that fractional order model (14) undergoes codimension-two bifurcation associated with 1:2, 1:3 and 1:4 strong resonances. In the case of 1:2 resonance, the system exhibits a resonance pattern where the frequency of one oscillatory component is twice that of another component. This can lead to the amplification or suppression of certain oscillations in the system, resulting in a complex behavior. In the case of 1:3 resonance, the system demonstrates a resonance pattern where the frequency of one oscillatory component is three times that of another component. Similar to the 1:2 resonance, this can lead to the amplification or suppression of specific oscillations and contribute to the emergence of intricate dynamics. In the case of 1:4 resonance, the system displays a resonance pattern where the frequency of one oscillatory component is four times that of another component. This resonance introduces further complexity to the system's behavior, affecting the amplitudes and phases of different oscillations.

Codimension-two bifurcations, such as the resonances mentioned above, provide insights into how different oscillatory modes interact and influence each other in the fractional-order cubic autocatalator model. The occurrence of these bifurcations can lead to the emergence of intricate dynamics, including chaotic behavior, multiple stable states, and complex oscillatory patterns. Understanding and characterizing these codimension-two bifurcations are essential for comprehending the system's behavior and its implications in chemical reactions and nonlinear dynamics.

In other words, the analysis of codimension-one and codimension-two bifurcations of a fractional-order cubic autocatalator chemical reaction system can help to understand the mechanisms and conditions for the emergence of complex dynamics in chemical reactions, and to control or manipulate them for practical purposes. For instance, some chemical reactions can be used to generate signals or patterns for communication or encryption. By tuning the fractional order or other parameters, one can switch between different modes of operation or enhance the security or robustness of the system.

References

[1] A. A. Alderremy, K. M. Saad, J. F. Gómez-Aguilar, S. Aly, D. Kumar, J. Singh, New models of fractional blood ethanol and two-cell cubic autocatalator reaction equations, *Math. Meth. Appl. Sci.* **46** (2023) 7767–7778.

[2] A. Mahecha-Botero, P. Garhyan, S. S. E. H. Elnashaie, Non-linear characteristics of a membrane fermentor for ethanol production and their implications, *Nonlin. Anal. Real World Appl.* **7** (2006) 432–457.

[3] A. Uppal, W. H. Ray, A. B. Poore, The classification of the dynamic behavior of continuous stirred tank reactors-influence of reactor residence time, *Chem. Eng. Sci.* **31** (1976) 205–214.

[4] A. M. A. El-Sayed, S. M. Salman, On a discretization process of fractional-order Riccati differential equation, *J. Fract. Calc. Appl.* **4** (2013) 251–259.

[5] B. F. Gray, M. J. Roberts, P. Gray, Analysis of chemical kinetic systems over the entire parameter space. I. The Sal'nikov thermokinetic oscillator, *Proc. Royal Soc. London A* **416** (1988) 391–402.

[6] B. F. Gray, R. A. Thuraisingham, The cubic autocatalator: the influence of degenerate singularities in a closed system, *J. Eng. Math.* **23** (1989) 283–293.

[7] C. Zhai, A. Palazoglu, S. Wang, W. Sun, Strategies for the analysis of continuous bioethanol fermentation under periodical forcing, *Ind. Eng. Chem. Res.* **56** (2017) 3958–3968.

[8] C. A. Pérez–Gómez, J. Espinosa, Design method for continuous bioreactors in series with recirculation and productivity optimization, *Chem. Eng. Res. Des.* **137** (2018) 544–552.

[9] C. Xu, D. Mu, Y. Pan, C. Aouiti, L. Yao, Exploring bifurcation in a fractional-order predator-prey system with mixed delays, *J. Appl. Anal. Comput.* **13** (2023) 1119–1136.

[10] C. Xu, Q. Cui, Z. Liu, Y. Pan, X. Cui, W. Ou, M. Rahman, M. Farman, S. Ahmad, A. Zeb, Extended hybrid controller design of bifurcation in a delayed chemostat model, *MATCH Commun. Math. Comput. Chem.* **90** (2023) 609–648.

[11] C. Xu, X. Cui, P. Li, J. Yan, L. Yao, Exploration on dynamics in a discrete predator-prey competitive model involving time delays and feedback controls, *J. Biol. Dyn.* **17** (2023) #2220349.

[12] C. Xu, Z. Liu, P. Li, J. Yan, L. Yao, Bifurcation mechanism for fractional-order three-triangle multi-delayed neural networks, *Neural Proc. Lett.* **1** (2022) 1–27.

[13] D. Mua, C. Xub, Z. Liua, Y. Panga, Further insight into bifurcation and hybrid control tactics of a chlorine dioxide-iodine-malonic acid chemical reaction model incorporating delays, *MATCH Commun. Math. Comput. Chem.* **89** (2023) 529–566.

[14] H. I. Abdel-Gawad, K. M. Saad, On the behaviour of solutions of the two-cell cubic autocatalator reaction model, *ANZIAM J.* **44** (2002) E1–E32.

[15] J. M. L. Corbel, J. N. J. Van Lingen, J. F. Zevenbergen, O. L. J. Gijzeman, A. Meijerink, Strobes: pyrotechnic compositions that show a curious oscillatory combustion, *Angew. Chem. Int. Ed.* **52** (2013) 290–303.

[16] J. H. Merkin, D. J. Needham, S. K. Scott, Oscillatory chemical reactions in closed vessels, *Proc. Royal Soc. London A* **406** (1986) 299–323.

[17] J. H. Merkin, D. J. Needham, S. K. Scott, On the creation, growth and extinction of oscillatory solutions for a simple pooled chemical reaction scheme, *SIAM J. Appl. Math.* **47** (1987) 1040–1060.

[18] L. N. Sridhar, Elimination of oscillations in fermentation processes, *AIChE J.* **57** (2011) 2397–2405.

[19] L. A. Leach, J. H. Merkin, S. K. Scott, Two-cell coupled cubic autocatalator: the effect of the uncatalysed reaction, *Dyn. Stab. Sys.* **7** (1992) 245–266.

[20] L. K. Forbes, C. A. Holmes, Limit-cycle behaviour in a model chemical reaction: the cubic autocatalator, *J. Eng. Math.* **24** (1990) 179–189.

[21] L. K. Forbes, Limit-cycle behaviour in a model chemical reaction: the Sal'nikov thermokinetic oscillator, *Proc. Royal Soc. London A* **430** (1990) 641–651.

[22] M. Chaplin, C. Bucke, *Enzyme Technology*, Cambridge Univ. Press, Cambridge, 1990.

[23] M. Y. Ongun, D. Arslan, J. Farzi, Numerical solutions of fractional order autocatalytic chemical reaction model, *Süleyman Demirel Univ. Fen Bilim. Enst.* **21** (2017) 165–172.

[24] M. E. E. Abashar, S. S. E. H. Elnashaie, Multistablity, bistability and bubbles phenomena in a periodically forced ethanol fermentor, *Chem. Eng. Sci.* **66** (2011) 6146–6158.

[25] N. Zhang, W. D. Seider, B. Chen, Bifurcation control of high-dimensional nonlinear chemical processes using an extended washout-filter algorithm, *Comput. Chem. Eng.* **84** (2016) 458–481.

[26] P. Gray, S. R. Kay, S. K. Scott, Oscillations of an exothermic reaction in a closed system. I. Approximate (exponential) representation of Arrhenius temperature-dependence, *Proc. Royal Soc. London A* **416** (1988) 321–341.

[27] P. Gray, S. K. Scott, Autocatalytic reactions in the isothermal, continuous stirred tank reactor: Oscillations and instabilities in the system $A + 2B \to 3B; B \to C$, *Chem. Eng. Sci.* **39** (1984) 1087–1097.

[28] P. Li, Y. Lu, C. Xu, J. Ren, Insight into Hopf bifurcation and control methods in fractional order BAM neural networks incorporating symmetric structure and delay, *Cognit Comput.* **1** (2023) 1–43.

[29] P. Li, X. Peng, C. Xu, L. Han, S. Shi, Novel extended mixed controller design for bifurcation control of fractionalorder Myc/E2F/miR-17-92 network model concerning delay, *Math. Methods Appl. Sci.*, in press, doi: `https://doi.org/10.1002/mma.9597`.

[30] Q. Zhao, H. Xu, L. Tao, Homogeneous-heterogeneous reactions in boundary-layer flow of a nanofluid near the forward stagnation point of a cylinder, *J. Heat Trans.* **139** (2017) #034502.

[31] Q. Din, M. S. Shabbir, M. A. Khan, A cubic autocatalator chemical reaction model with limit cycle analysis and consistency preserving discretization, *MATCH Commun. Math. Comput. Chem.* **87** (2022) 441–462.

[32] Q. Din, U. Saeed, Stability, discretization and bifurcation analysis for a chemical reaction system, *MATCH Commun. Math. Comput. Chem.* **90** (2023) 151–174.

[33] Q. Din, Dynamics and Hopf bifurcation of a chaotic chemical reaction model, *MATCH Commun. Math. Comput. Chem.* **88** (2022) 351–369.

[34] Q. Din, A novel chaos control strategy for discrete-time Brusselator models, *J. Math. Chem.* **56** (2018) 3045–3075.

[35] Q. Din, Bifurcation analysis and chaos control in discrete-time glycolysis models, *J. Math. Chem.* **56** (2018) 904–931.

[36] Q. Din, T. Donchev, D. Kolev, Stability, bifurcation analysis and chaos control in chlorine dioxide-iodine-malonic acid reaction, *MATCH Commun. Math. Comput. Chem.* **79** (2018) 577–606.

[37] Q. Din, K. Haider, Discretization, bifurcation analysis and chaos control for Schnakenberg model, *J. Math. Chem.* **58** (2020) 1615–1649.

[38] R. J. Field, R . M. Noyes, Oscillations in chemical systems. IV. Limit cycle behavior in a model of a real chemical reaction, *J. Chem. Phys.* **60** (1974) 1877–1884.

[39] S. R. Kay, S. K. Scott, Oscillations of simple exothermic reactions in a closed system. II. Exact Arrhenius kinetics, *Proc. Royal Soc. London A* **416** (1988) 343–359.

[40] W. Ou, C. Xu, Q. Cui, Z. Liu, Y. Pang, M. Farman, S. Ahmad, A. Zeb, Mathematical study on bifurcation dynamics and control mechanism of tri-neuron BAM neural networks including delay, *Math. Methods Appl. Sci.*, in press doi: `https://doi.org/10.1002/mma.9347`.

[41] X. Zhao, W. Marquardt, Reactor network synthesis with guaranteed robust stability, *Comput. Chem. Eng.* **86** (2016) 75–89.

[42] Y. A. Kuznetsov, *Elements of Applied Bifurcation Theory*, Springer, New York, 2004.